Residual stress control during the growth and release process in gold suspended microstructures

Akshdeep Sharma*[a], Deepak Bansal[a], Amit Kumar[a], Dinesh Kumar[b], Kamaljit Rangra[a]

[a]Sensors and Nanotechnology Group, Central Electronics Engineering Research Institute (CEERI)/ Council of Scientific and Industrial Research (CSIR), Pilani, Rajasthan, India,
[b]Dept. of Electronic Science, Kurukshetra University, Kurukshetra, Haryana, India,

ABSTRACT

This paper presents the growth and release process effects on the deformation of suspended gold micro-structures. Cantilever type test structures, typically used for RF MEMS devices have been examined. The structures have a thickness of 2µm, produced by patterned gold electro deposition above a sacrificial photoresist layer, then removed by dry release in oxygen plasma ashing and wet release using critical point dryer (CPD). The growth process of gold electroplating is optimized for low residual stress using pulse power supply. Minimum stress 35-60 MPa is obtained at grain size 30-45nm and RMS roughness of the order of 5-8nm. The growth mechanism of structural layer and releasing methods are optimized to obtain planar MEMS structures. The main parameters considered are the initial stress during the growth of electroplated gold and the release process recipes developed for fabrication of metallic structural layer.

Keywords: RF MEMS, Plasma ashing, Critical Point Dryer (CPD), Electroplating, Microstructure, Deformation

1. INTRODUCTION

In view of the role of stress in MEMS (micro-electro-mechanical systems) device design, functioning and reliability, the identification and characterization of residual stress in MEMS structures is of paramount importance. From the device perspective, the existence of residual stresses[1] essentially changes the performance and reduces the structural integrity and lifetime of MEMS devices. Therefore, in the MEMS device design one must predetermine and control the residual stress levels to obtain functional tolerances or to prevent total structural failure of a mechanical design. The existence of stress in thin film metallic structures used in most of the MEMS structures, leads to a change in effective stiffness, warping, local deformation or cracking of films in extreme cases. This severely undermines the device reliability and precision in terms of device parameters such as actuation voltage, s-parameters, natural mechanical frequency, and quality factor. On the other hand MEMS based techniques and devices provide a new tool for studying the mechanical properties of materials[2] such as Young's modulus, hardness, and state of stresses[3]. As a result, MEMS test structures[4] have a very significant role in characterization of the mechanical properties (residual stress in particular) of MEMS devices and materials. In particular, stress and stress gradient are strongly dependent on deposition conditions, thermal treatments and other process dependent variables[5].

In general, metals can be used in MEMS fabrication; gold is very attractive especially for RF MEMS devices, because of its high conductivity that helps reducing the losses, also for its chemical inertness that prevents contamination and corrosion problems. Gold is not an excellent material from the mechanical point of view, and its yield, creep and thermal relaxation properties are often source of high stresses and important homogeneities in the stress distribution. Electroplated gold thin films are commonly used for the MEMS devices as they provide a simple and cheap technology with superior material properties and device performances.

*akshdeepsharma@gmail.com Phone 91 1596 252218; fax 91 1596 242294; www.ceeri.res.in

Micromachining and Microfabrication Process Technology XIX, edited by Mary Ann Maher, Paul J. Resnick,
Proc. of SPIE Vol. 8973, 89730F · © 2014 SPIE · CCC code: 0277-786X/14/$18 · doi: 10.1117/12.2041433

Various MEMS devices such as pressure sensors, MEMS switches, microcoils, micromotors and microstructures based on plated metals have been fabricated and studied[16-22]. However, electroplated MEMS structures usually exhibit large deflections after the plasma ashing process, which is frequently used to release the MEMS structures from the substrate. The present study quantitatively analyses the electroplating growth mechanism and deformations of electroplated Au MEMS structures released by plasma ashing, CPD and investigate the possible causes of the deformations.

2. ORIGIN AND MEASUREMENT OF RESIDUAL STRESS

2.1 Thin film stress

The origin of stresses in thin films, microelectronics, and MEMS structures has been reviewed extensively by many researchers [1, 2]. Fundamentally, it can be classified into two major categories, the mismatch between thermomechanical properties of materials and the thin-film deposition or growth generated intrinsic stress. Thermal stresses are induced due to strain misfits, as a result of differences in the temperature dependent coefficient of thermal expansion between the thin film and a substrate material such as silicon, photoresist, gold etc. Intrinsic stresses are generated due to strain misfits encountered during phase transformation in the formation of a solid layer of a thin film. Residual or internal thin film stress therefore can be defined as the summation of the thermal and intrinsic thin film stress components[2]

$$\sigma_R = \sigma_T + \sigma_I \tag{1}$$

where σ_R is the residual stress, σ_T is the thermal stress component, σ_I is the intrinsic stress component.

Simple mechanics of materials are therefore employed to study the mechanical residual stress induced in thin films. After a film is deposited onto a substrate at an elevated temperature, it cools down to a room temperature. When the film/substrate composite is cooled, they contract with different magnitudes because of different coefficients of thermal expansion between the film and the substrate. The film is subsequently strained elastically to match the substrate and remain attached, causing the substrate to bend. This along with the intrinsic film stress developed during film growth, gives rise to a total residual film stress [2-9].

2.2 Stress reduction during growth of layer

Residual stress control during the layer growth is an important process step. Growth mechanism strongly influences the in built stress. Electroplating process nucleation stages are shown in SEM micrographs in figures 3, from micrographs gold particle grain size range is measured from 20 -70nm.The stress measurement of the electrodeposit gold layer of 2µm thick is carried out using curvature measurement method as mentioned in next section. Initially electroplating is processed using DC power supply with varying current density and corresponding thickness, roughness, grain size and residual stress is measured. Same experiments are explored using pulse power supply; the purpose of the pulse supply is reducing the grain size and residual stress. The grain size and roughness is measured using AFM and XRD.

2.2.1 Grain Size measurement

According to Scherer's equation grain size can be measured using XRD data peak. The governing equations are as follows:

Crystalline Size $$D = \frac{K\lambda}{B\cos\theta} \tag{2}$$

Microstrain $$\varepsilon = \frac{B\cos\theta}{4} \tag{3}$$

Estimation of number of crystallites $$N = \frac{t}{D^3} \tag{4}$$

Where λ: X-ray wavelength (1.54178Å), B is the full width at half maximum, θ Bragg's angle, t film thickness and K constant average value (0.9). Figure 6(a) shows XRD peak for 2µm thick plated gold film after deposition and 6(b) shows after annealing at 150^0C. XRD peak are used to find out grain size using equation 2 and crystalline orientation of Au deposit layer[18]. Grain sizes are further verified using AFM data. Finer grain size and reduced roughness deposit using

pulse power supply also measured using AFM and XRD as shown in figure 4 (b).The extracted parameters of electroplated gold for minimum residual stress, fine grain size and roughness are finalize. The resultant optimized plating recipes are used for fabricating single clamped cantilever structures as well as RF MEMS switches.

2.3 Stress measurements by substrate curvature method

The most widely acknowledged thin film stress measurement method is the curvature measurement of beam or plates structures. For beam structures, consider a composite film-substrate beam of width *b*. The film thickness and Young's modulus are t_f and E_f respectively, and the corresponding substrate values are t_s and E_s. In the free body diagram of each set of interfacial forces can be replaced by the statically equivalent combination of a force and moment F_f and M_f in the film, F_s and M_s in the substrate, where $F_f = F_s$. Force F_f can be imagined to act uniformly over the film cross section ($t_f b$) giving rise to the film stress. The moments are responsible for the bowing of the film-substrate composite. By counting the biaxial state of stress and the final equation[11] becomes

$$\sigma_f = \frac{F_f}{t_f b} = \frac{1}{6R}\frac{E_s t_s^2}{(1-\nu_s)t_f} = \frac{1}{6(R_f - R_i)}\frac{E_s t_s^2}{(1-\nu_s)t_f} \tag{5}$$

Equation 5 is the standard Stoney's formula to find out residual stress of the deposit layer, by measuring the radius of curvature (R) , before (R_i) and after (R_f) the thin film deposition on full wafer. The residual stress in the 2µm plated Au layer is between 100 -120MPa[14].

2.4 Residual Stress Gradient measurement using cantilever

The residual stresses of MEMS films usually vary in the thickness direction. A zero mean residual stress does not imply a satisfactory situation. Once the film is released by sacrificial etch, the mean residual stress vanish but the non-uniformity of the residual stress actually cause an out of plane deformation. As shown in figures 7, this out of plane deformation can cause performance degradation in MEMS devices such as RF switches.

The uniformity of stress through the depth of a film introduces an important property to control. Variations in the magnitude and direction of the stress in the vertical direction can cause cantilever structures to curl toward or away from the substrate. Stress gradients present in MEMS films must be controlled to ensure predictable behavior of designed structures when released from the substrate[12]. To determine the residual stress, non-contact surface profilometer measurements for tip deflection is used on an array of simple cantilever beams. The stress gradient can be extracted from the deflection amplitude of different suspended cantilevers[13]. When the structure is released, the stress σ_0 is relaxed and the stress gradient acts on the beam. The bending moment due to the stress gradient is written as:

$$M = \int_{-t/2}^{t/2} zb\sigma(z)dz \tag{6}$$

Where *b* is the beam width, and z the coordinate in the thickness direction. The stress gradient σ' is defined as

$$\sigma' = M/EI \tag{7}$$

From beam theory for a cantilever with an applied end moment, the tip deflection due to the presence of the stress gradient is

$$\delta tip = \frac{ML^2}{2EI} = \frac{\sigma' L^2}{2} \tag{8}$$

Eq. (9) shows the correlation of the tip deflection of the cantilever beam and the maximum stress on the beam cross-section[24].

$$\sigma_{max} = \frac{\sigma' t}{2} = \frac{\delta_{tip} tE}{L^2} \tag{9}$$

The displacement at the tip of the cantilever is measured with an optical profiler. The stress gradient $3.48\times10^{-4}\mu m^{-1}$ is extracted from the fit of the tip deflection versus the cantilever length[14]. Equation 9 is used to calculate maximum residual stress. The anchor effect[24] is not considered in the equation 9.

3. FABRICATION PROCESS STEPS

Figure 1 shows the schematic view of process steps for MEMS cantilever as a part of RF MEMS switch fabrication[16, 17]. A set of microstructures were realized using surface micromachining techniques, on a 2″ diameter P-type <100> oriented silicon wafer. A thermal oxide was grown on the substrate, then a 3.5µm positive tone photoresist HiPR 6517 was deposited and patterned as a spacer layer. The main advantage of this PR is that after baking at 180^0C, it becomes hard plastic like structure with edges suitable for conformal metal coating. A seed layer of Ti/Au is deposited by sputtering. This is followed by lithography of AZ 9260 photoresist for bridge mold formations. Gold electroplating of 2µm thick is obtained at current density 3.5mA/cm^2 and temperature 60^0C for 10 minutes using sulphite gold (TSG 250) electrolyte. After the removal of PR mold and Au/Ti seed layers, microstructures are released by CPD and plasma ashing process. A layout of the cantilevers studied in this paper is reported in figure 2 (a-c), three cantilevers series with the same shape but with different dimensions (fig. 2 a, b and c). In the first cantilever series the length goes from 40 to 280µm and the width is 20µm while in the second cantilever series the length goes from 25 to 500 µm and the width is 30µm and in third cantilever series with actuation electrode length goes from 150-500µm and width is 30µm. The suspended parts are of gold color. The area originally covered by the spacer has been marked with a dashed line (gray color). These structures are representative of typical single-clamped microstructures encountered in MEMS fabrication. The devices have been distributed in several locations on the wafer layout to check the process uniformity on wafer.

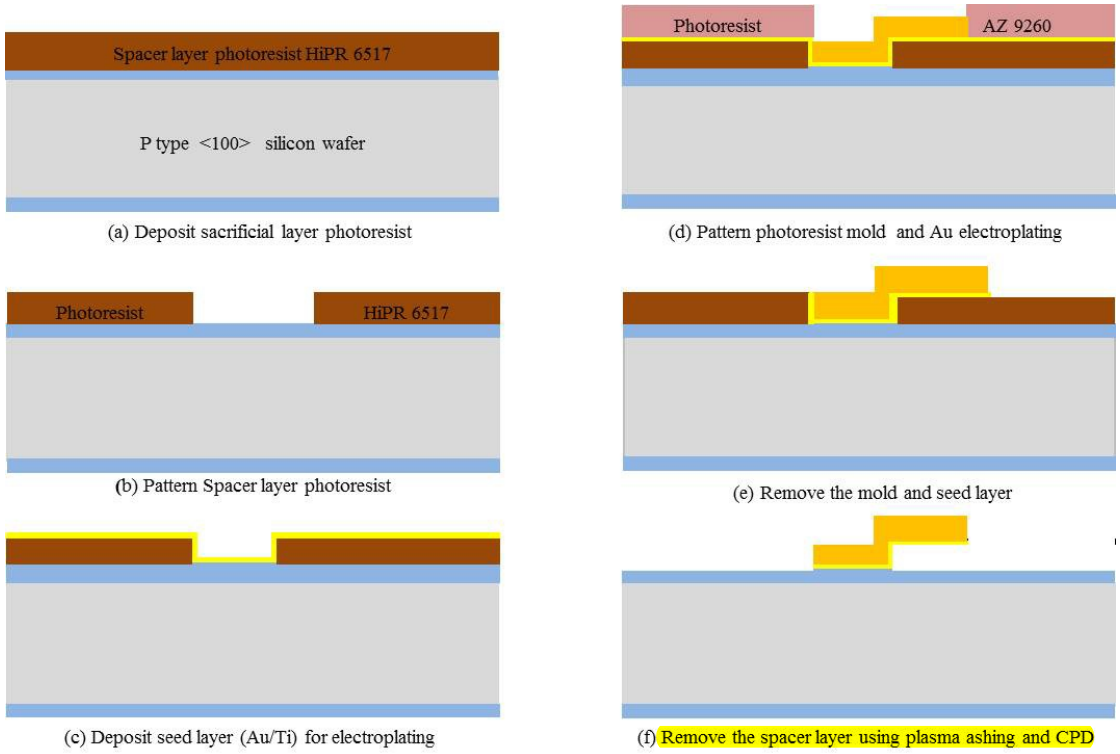

Figure 1 (a)- (f) Fabrication process steps for electroplated MEMS cantilever

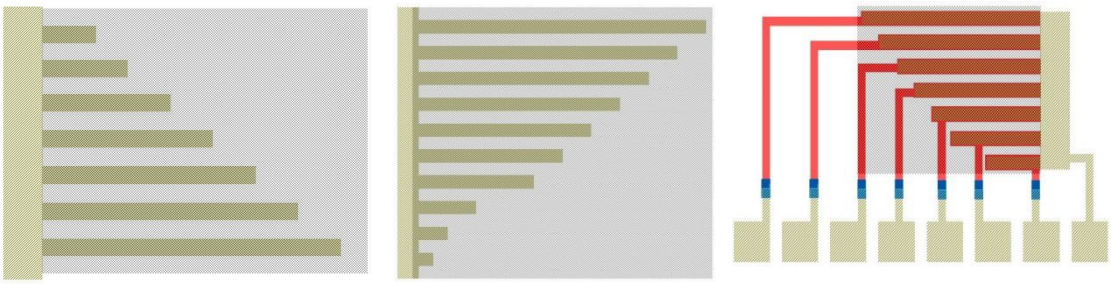

Figure2 (a) Narrow gold cantilever array (b) Large gold cantilever (c) Cantilever array with actuation electrode

4. RESULTS AND DISCUSSION

4.1. The growth process

The electroplated gold layer growth process is start with the observations of nucleation stage, this is observed using SEM after gold plating for 5-10 second at current density 3.5mA/cm^2 and temperature 60^{0}C. SEM micrographs at different magnification is shown in figure 3, it shows that average grain size of gold varies from 20-70nm. Current density impact on DC plated Au is measured using AFM shown in figure 4(a). Pulse plating effect on grain size and roughness with duty cycle is shown in figure 4(b). Residual stress is measured using curvature method for DC and pulse plating shown in figure 5(a-b). The minimum stress obtained using pulse plating is 35 -60 MPa at duty cycle 5-15% respectively.

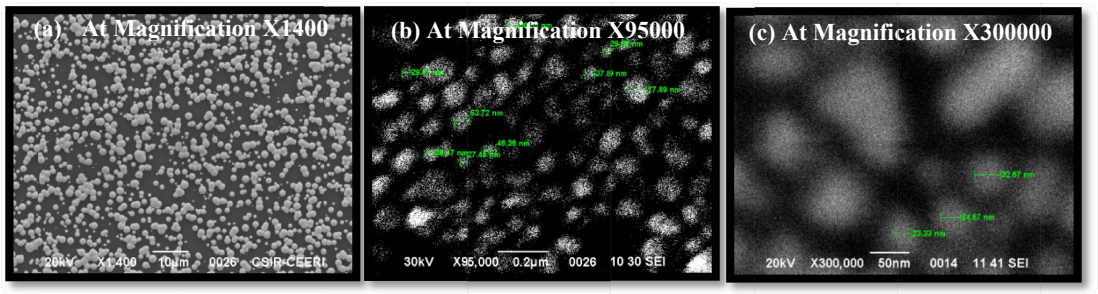

Figure 3 Gold Electroplating nucleation stages with average grain size varies from 20-70nm

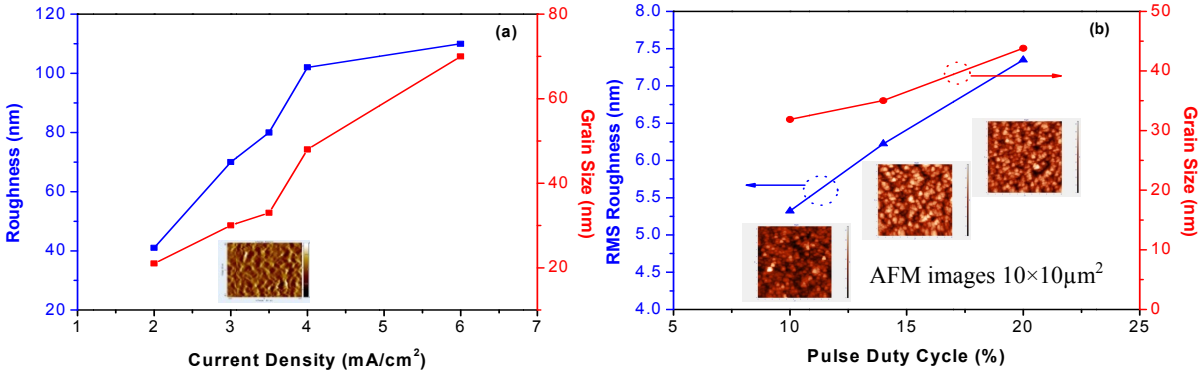

Figure 4 (a) DC gold plating current density and (b) Pulse duty cycle effect on grain size and roughness

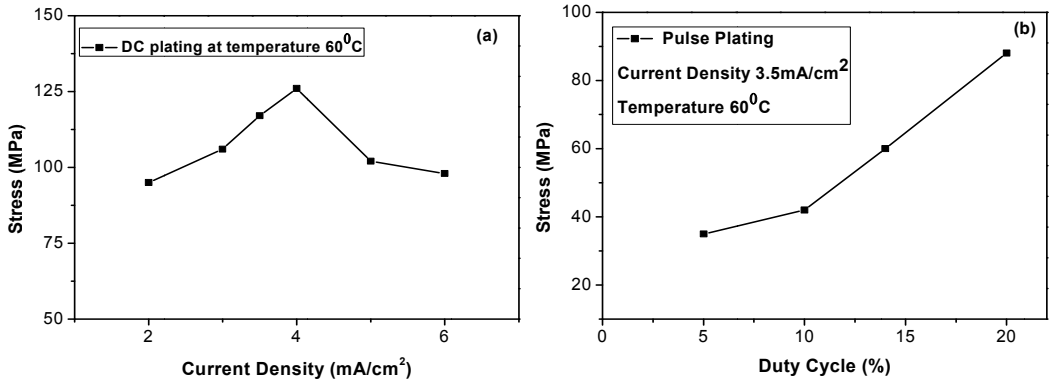

Figure 5(a) DC gold plating current density and (b) Pulse plating duty cycle effect on residual stress

The XRD peaks of pulse plated gold are shown in figure 6(a), the result shows highest intensity for Au (111). Annealing of plated layer is done at 150^{0}C for 30 minutes to observe the shift in peak intensity. Au (220) peak intensity is higher after annealing as shown in figure 6(b). The grain size measured using equation 2 is 31.86nm for XRD data of figure 6(a). The crystalline orientation (111) is dominating XRD peak of pulse pated gold after deposition.

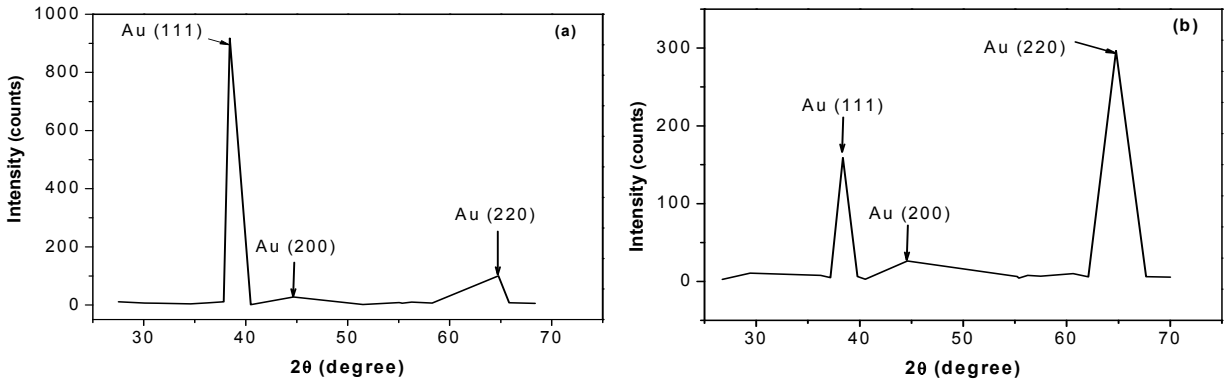

Figure 6(a, b) XRD patterns of plated Au film before and after annealing at a temperature of 150^0C.

4.2. The release process

The tip deflection of the released MEMS cantilever beam is measured after dry-etching the sacrificial layer with plasma ashing, and the residual stress is obtained based on the analytical model expressed in equation 9. The 'Drytek mega strip 6 HF' plasma asher which performs an isotropic dry etch of the PR with oxygen plasma, is used for dry release process. As the oxygen plasma (at 900watts) was inefficient in removing the hard crust of the PR baked at 180^0C. For the crust removal, a combination of oxygen and CF_4 was supplied to the plasma chamber in a ratio of 35:1, process details available in our publication[25]. Table 1 shows the recipes of the dry etching process used in the present study. To maintain the stable plasma etching condition, the minimum process time is experimentally determined as 10 min., after 3 min. in CF_4 and O_2 plasma for hard crust removal. The deformation characteristics with the etching condition of a single ashing process without break are excluded due to too large plastic deformation of the cantilever resulting damage of microstructure.

Meanwhile, the residual stress causing the tip deflection of the MEMS structures can be generated not only in the plasma ashing process but also in the film deposition process. In order to evaluate the residual stress generated during the deposition process, the MEMS cantilever beam is released by removing the sacrificial layer with wet etching and the tip deflection is measured. The wet etching air dry and CPD release is also explored for cantilever structures in the present paper. Table 1 shows the recipe for wet etching process using CPD. Figure 7 (a-c) shows the SEM images of the released MEMS structures with 3D optical profiler images.

4.3 Tip deflection and the residual stress

As shown in the figures 8 (a-c), the cantilever beams released by wet etching (CPD) shows small tip deflections while those released by plasma ashing show considerable amounts of tip deflections. The magnitude of the tip deflection of the cantilever beam released by plasma ashing seems to be dependent on the total process time as well as the step process time of plasma ashing. The detailed process time for each case is listed in Table 1.

Table 1 shows two cases of plasma ashing and two cases of wet etching air and CPD. The plasma ashing consists of a case 1: O_2 plasma at low RF power of 80 watt for total process time of 410 minutes, case 2: Initial $CF_4 + O_2$ plasma for hard crust removal, followed by O_2 plasma step process time (10 min. on) and break time (10 min. off) at RF power 900watt for total process time 90 minutes. Plasma ashing case 1 has the long step process time in oxygen plasma; Case 2 has the short step process time as well as the short total process time. Case 1, with the long step process time, yields a larger deflection than in case 2 having the short step process time. Figures 8 shows the tip deflections of the MEMS cantilever beams of various lengths, where the tip deflections are measured by 3D optical profiler. The cantilever beams released by plasma ashing shows large deflections while those released by the wet etching CPD and air drying shows small deflections, regardless of the beam length. Wet release air drying structures have a problem of non-uniform deflection due to stiction to substrate, as this technique only suitable for high stiffness structures. Overall tip deflection of CPD released microstructures is 3-12µm as shown in figure 8 (a).

Figure 9(a-c) shows the maximum residual stresses calculated from the measured tip deflections of the MEMS cantilever beams. The analytical model expressed in equation 9 is utilized to evaluate the maximum residual stresses[24] and the value of Young's modulus is set to 80 GPa and thickness 2µm of gold material. The residual stresses of the cantilever beams released by the CPD are small. Figure 9 also shows that case 1 has the highest residual stress, which confirms that

the length of the step process time in the plasma ashing process is a very critical factor in the residual stresses of the MEMS structures.

Table 1 Process parameters for dry and wet release of microstructures.

Dry Release				**Wet Release**		
Sacrificial Photoresist		HiPR 6517		HiPR 6517		
Process parameters		**Case1**	**Case 2**	Process parameters	**Case 1**	**Case 2**
RF power		80watt	900watt	Release Methods	Supercritical CPD	Air drying
Operating Pressure (m torr)		112	400	Procedure	Mild piranha » DI water » IPA	
Etch Rate (nm/min)	Vertical	14-35	230-350	Critical Pressure (Co_2)	1072Pa	N/A
	Lateral	8-11	38-77			
Ashing process		O_2 [100%]	CF_4[20%]+O_2[80%], O_2 [100%]	Critical temperature (Co_2)	31.1^{0}C	N/A
Process time (min.)		410	90 (10 on + 10 off)	Process time (min.)	30	60

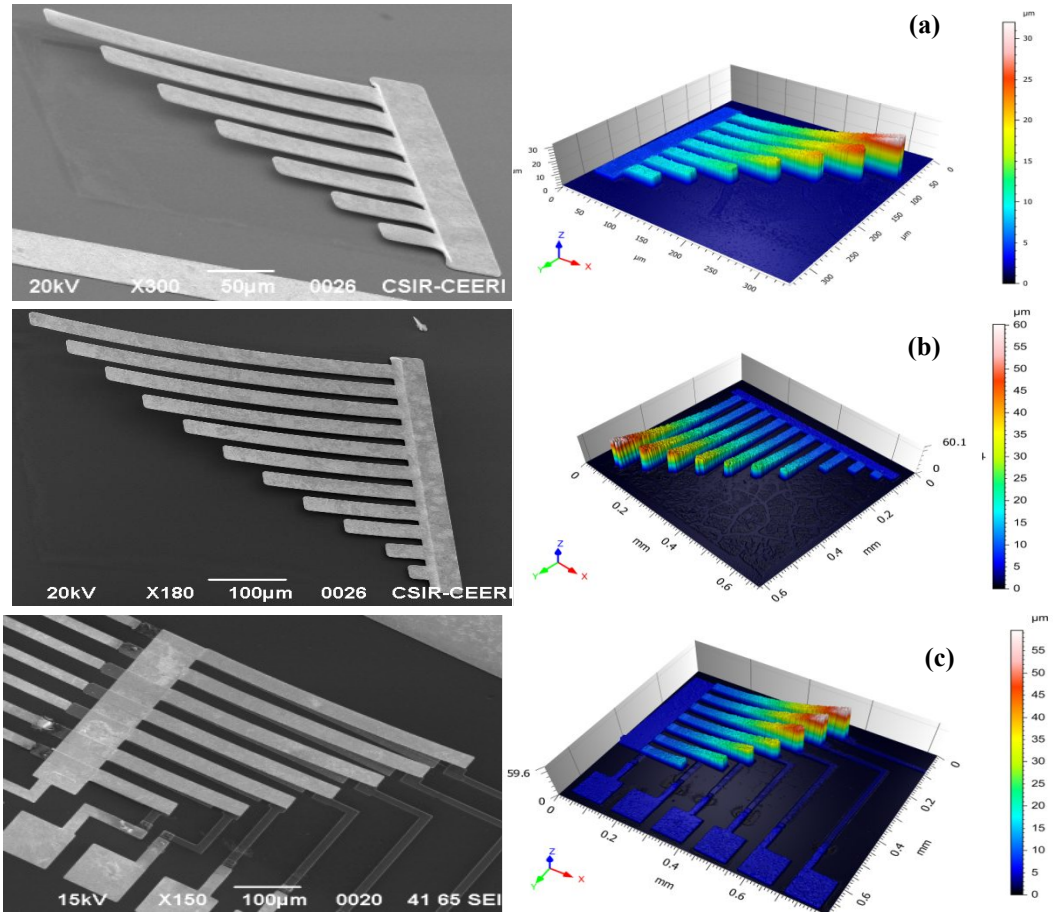

Figure 7 (a, b and c) SEM and 3D optical profile of cantilever tip deflection of the released structure.

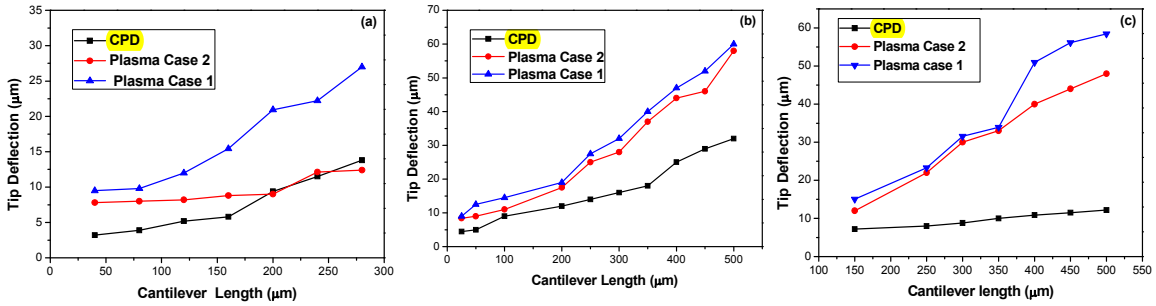

Figure 8 (a, b and c) Tip deflection of the released structures w.r.t. cantilever length.

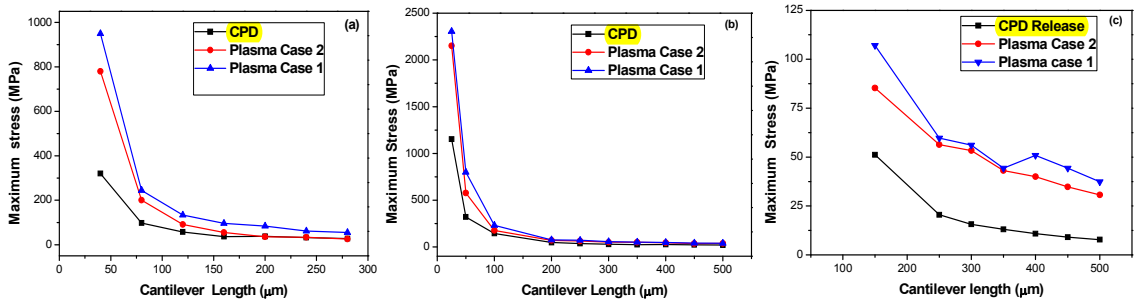

Figure 9 (a, b and c) Maximum residual stress of released microstructures w.r.t. cantilever length.

CONCLUSIONS

The flexural deformation of the electroplated MEMS structures after plasma ashing and CPD released are quantitatively analysed. The main causes of cantilever deflection are residual stress during growth and releasing method of sacrificial layer. Material anisotropy in the thickness direction that was created during the deposition process is another cause of the deflection of the MEMS structures. The minimum stress (35- 60 MPa) is obtained at fine grain size (30-45nm) using pulse power supply. The deflection of the released MEMS structure in dry release is generated due to the plasma environment, small steps ashing time (10 min. on, off) minimise deformation effect up to some extent. CPD released structure shows minimum deformation and residual stress. Finally, changes in the surface microstructures and composition of the gold layer are considered to be dominant factors in generating deformation of the electroplated MEMS structures.

ACKNOWLEDGMENTS

Authors would like to acknowledge Director, CSIR - CEERI, Pilani, for providing the design and fabrication facilities and CSIR New Delhi and NPMASS for financial support. The authors would also like to thank all the members of Sensors and Nanotechnology group for their help in fabrication of the devices.

REFERENCES

[1] M.F. Doerner , W.D. Nix , “Stresses and deformation processes in thin films on substrates” , CRC Crit. Rev. Solid State Mater. Sci. 14, 225 (1988)

[2] W.D. Nix, “Mechanical properties of thin films”, Metall. Trans. 20A, 2217 –2245 (1989)

[3] S.M. Hu, “Stress related problems in silicon technology”, J. Appl. Phys. 70, R53– R80 (1991)

[4] R.W. Hoffman, “Stresses in thin films: The relevance of grain boundaries and impurities”, Thin Solid Films 34, 185 (1976)
[5] J. Lu (Ed.), [Handbook of Measurement of Residual Stresses], Fairmont Press ,Liburn, GA , (1996)
[6] P.J. Withers , H. Bhadeshia ,“Residual stress part I – measurement techniques” , Mater. Sci.Technol. 17, 355 – 365 (2001)
[7] P.J. Withers , H. Bhadeshia ,“Residual stress part 2 – nature and origins” , Mater. Sci. Technol. 17, 366 – 375 (2001)
[8] F.A. Kandil, J.D. Lord, A.T. Fry, P.V. Grant, “A review of Residual Stress Measurement Methods – A Guide to Technique Selection” NPL Report MATC(A)04, UK, (2001)
[9] Akshdeep Sharma, Maninder Kaur, Deepak Bansal, Dinesh Kumar, Kamaljit Rangra, “Review of MEMS test structures for mechanical parameter extraction”, J. Nano-Electron. Phys., 3, No. 1, 243-253 (2011)
[10] John A. Thornton D. W. Hoffman “Stress-related effects in thin films” Thin Solid Films, 171, 5-31 (1989)
[11] Stoney, G.G. **“**The tension of metallic films de-posited by electrolysis”, Proc. Royal Soc. London, A82, 172-175 (1999)
[12] Senturia, S.D. [Microsystem design], Kluwer Academic Publishers, Norwell, MA, 183-237 (2002)
[13] Fang, W.; Wickert, J.A. **“**Determining mean and gradient residual stresses in thin films using micromachined cantilevers”, J. Micromechan. Microeng. 6(3), 301-309 (1996)
[14] Akshdeep Sharma et. al, “Fabrication and Analysis of MEMS Test Structures for Residual Stress Measurement”, Sensors & Transducers, 13, 21-30 (2011)
[15] Akshdeep Sharma, Deepak Bansal, KamaljitRangra , Dinesh Kumar “A Test Structure for in-situ Determination of Residual Stress”, UACEE International Journal of Advances in Electronics Engineering Volume 2: Issue 3 139-142 (2012)
[16] K. Rangra et. al, “STS - a new type of RF MEMS Switch for Telecom. Applications: Design and fabrication”, Sensors and Actuators A, 123-124, 505-514(2005)
[17] Deepak Bansal, Amit Kumar, Akshdeep Sharma, Prem Kumar and K.J. Rangra “Design of Novel compact anti-stiction and low insertion loss RF MEMS switch”, Accepted in Microsystem Technologies Volume 19, Number 5 May (2013)
[18] Wu Tang, KeweiXu, Ping Wang, Xian Li “Residual stress and crystal orientation in magnetron sputtering Au films”,Materials Letters 57 3101– 3106, (2003)
[19] S.D. Leith, D.T. Schwartz, “High-rate through-moldelectrodeposition of thick (>200μm) NiFe MEMS components with uniform composition”, J. Microelectromech. Syst. 8, 384–392 (1999)
[20] J. Gobet, F. Cardot, J. Bergqvist, F. Rudolf, “Electrodeposition of 3D microstructures on silicon”, J. Micromech. Microeng. 3, 123–130 (1993)
[21] S. Majumder, N.E. McGruer, P. Zavracky, “Electrostatically actuated micromechanical switches”, J. Vac. Sci. Technol. A 15,1246–1249 (1997)
[22] K. Kataok, S. Kawamura, T. Itoh, K. Ishikawa, H. Honma, T. Suga, “Electroplating Ni micro-cantilevers for low contact-force IC probing”, Sens. Actuators A, Phys. 103,116–121 (2003)
[23] V. Mulloni, F. Giacomozzi, B. Margesin, ”Controlling stress and stress gradient during the release process in gold suspended micro-structures”Sensors and Actuators A 162, 93–99 (2010)
[24] T.J. Kang, J.G. Kim, J.H. Kim, K.C. Hwang, B.W. Lee, C.W. Baek, Y.K. Kim, D. Kwon, H.Y. Lee, Y.H. Kim, “Deformation characteristics of electroplated MEMS cantilever beams released by plasma ashing” Sensors and Actuators A 148, 407–415 (2008)
[25] Akshdeep Sharma, Prachi Jhanwar, Deepak Bansal, Amit Kumar, Maninder Kaur, Shilpi Pandey, Prem Kumar, Dinesh Kumar, and Kamaljit Rangra “Comparative Study of Various Release Methods for Gold Surface Micromachining” Accepted in Journal of Micro/Nanolithography, MEMS, and MOEMS (JM3), January(2014)